SUPPORTING INFORMATION FOR

Piezoelectric Nanoparticle-Assisted Wireless Neuronal Stimulation

Attilio Marino[1,2,], Satoshi Arai[3], Yanyan Hou[3], Edoardo Sinibaldi[1], Mario Pellegrino[4], Young-Tae Chang[5,6], Barbara Mazzolai[1], Virgilio Mattoli[1], Madoka Suzuki[3,7,*], Gianni Ciofani[1,*]*

[1]Center for Micro-BioRobotics, Istituto Italiano di Tecnologia, Viale Rinaldo Piaggio 34, 56025 Pontedera (Pisa), Italy

[2]The Biorobotics Institute, Scuola Superiore Sant'Anna, Viale Rinaldo Piaggio 34, 56025 Pontedera (Pisa), Italy

[3]WASEDA Bioscience Research Institute in Singapore (WABIOS), Biopolis Way 11, #05-02 Helios, 138667 Singapore

[4]Dipartimento di Ricerca Traslazionale e delle Nuove Tecnologie in Medicina e Chirurgia University of Pisa, Via Savi 10, 56126 Pisa, Italy

[5]Department of Chemistry, National University of Singapore, MedChem Program of Life Sciences Institute, National University of Singapore, 3 Science Drive 3, 117543 Singapore

[6]Laboratory of Bioimaging Probe Development, Singapore Bioimaging Consortium, Agency for Science, Technology and Research (A*STAR), Biopolis, 138667 Singapore

[7]Organization for University Research Initiatives, Waseda University: #304, Block 120-4, 513 Waseda-Tsurumaki-Cho, Shinjuku-Ku, 162-0041 Tokyo, Japan

[*]attilio.marino@iit.it; suzu_mado@aoni.waseda.jp; gianni.ciofani@iit.it

S1. Estimate of the voltage generated on a BTNP subjected to ultrasounds

With reference to the experimental conditions detailed in the present study, we aimed at assessing whether ultrasounds (US) could induce voltage values up to a few mV, as typically required for activating voltage-sensitive membrane channels.[S1] To the purpose, we estimated the maximum voltage generated on the surface of a single barium titanate nanoparticle (BTNP), so as to possibly recall the superposition principle for those regions on the cell membrane where nanoparticles cluster (see Figure 2b). We hereafter report a simple electro-elastic model that permits to estimate the sought voltage. We also show that, based on the model predictions, channel activation can be effectively achieved by using higher US intensities (namely 0.8 W/cm^2), in full agreement with the experimental observations.

Modeling approach and working assumptions

In light of the involved length-scales (10^3 μm for the US transducer and for the cell-transducer distance; 10 μm for the cell diameter; 1 μm for the cell thickness; 10^{-1} μm for the BTNP diameter) and time-scales (1 MHz for the US waves), the cell is essentially subjected to a plane wave (so that no major conformational changes are expected on the membrane due to the US action), and each BTNP "feels" a uniform – yet time-varying – pressure on its surface. Moreover, the pressure variation can be regarded to as quasi-static, since the US frequency is several orders of magnitude smaller than the resonance frequency of the BTNP. Indeed, the fundamental frequency for a free spherical nanoparticle (NP) with radius R is $f \approx \frac{\left(\frac{E}{\rho}\right)^{\frac{1}{2}}}{2\pi R}$, where E and ρ respectively denote the Young modulus and the density of the NP.[S2-S3] For the present

study $R = 1.5 \cdot 10^{-7}$ m. Moreover, $\rho \cong 6 \cdot 10^3$ kg/m^3 [S4] and $E \cong 70$ GPa;[S5-S6] both values are derived from the ones of bulk barium titanate, and the adopted Young modulus was used in previous studies specifically addressing piezoelectric nanostructures. Hence, for our BTNP we obtain $f \approx 1$ GHz, and this value is not significantly altered by the contact with the cell membrane.[S3]

Based on the above considerations, let us simplify the problem by studying the voltage induced on a free BTNP by an external pressure p_{US}. To the purpose, we assume the BTNP to be spherical, homogeneous, isotropic, and linearly elastic. This way, we can tackle a simplified spherical symmetric problem and look for an analytical solution (which is hardly viable without invoking symmetry[S7-S9]). Indeed, in spite of the inherent simplifications, we look for an explicit solution able to account for the physically-representative effects.

Model formulation

Let us invoke the spherical symmetry to simplify the formulation. As regards the stress tensor (and with reference to the standard spherical coordinates r, θ and ϕ), we need to only consider $\sigma_r(r)$ and $\sigma_\theta(r)$, and the equilibrium reads:[S10]

$$\dot{\sigma}_r + 2\frac{\sigma_r - \sigma_\theta}{r} = 0, \tag{S1}$$

where the dot operator hereafter denotes differentiation with respect to r. Furthermore, the electric displacement is divergence-free, so that its only component D_r is such that $r^2 D_r$ does not depend on r. For the solution not to be singular at $r = 0$, we have $D_r = 0$.

The piezoelectric constitutive equations then read:[S8]

$$\sigma_r = c_{rr}\dot{u} + 2c_{r\theta}\frac{u}{r} + e_{rr}\dot{\varphi}, \tag{S2}$$

$$\sigma_\theta = c_{r\theta}\dot{u} + (c_{\theta\theta} + c_{\theta\phi})\frac{u}{r} + e_{r\theta}\dot{\varphi}, \tag{S3}$$

$$D_r = e_{rr}\dot{u} + 2e_{r\theta}\frac{u}{r} - \varepsilon_{rr}\dot{\varphi}\,, \tag{S4}$$

where u denotes the radial displacement (*i.e.*, the only component of the displacement field), and φ indicates the electric potential. Moreover, c_{rr}, $c_{r\theta}$, $c_{\theta\theta}$ and $c_{\theta\phi}$ are the elastic constants, e_{rr} and $e_{r\theta}$ denote the piezoelectric coefficients, and ε_{rr} represents the dielectric constant.

Furthermore, by recalling classical relations from linear elasticity,[S10] the elastic constants appearing in Eq. (S2-S3) can be recast as follows:

$$c_{rr} = c_{\theta\theta} = \frac{E}{(1+\nu)(1-2\nu)}(1-\nu) \tag{S5}$$

$$c_{r\theta} = c_{\theta\phi} = \frac{E}{(1+\nu)(1-2\nu)}\nu\,, \tag{S6}$$

where ν represents the Poisson ratio. Hence, the elastic constants are hereafter understood as known expressions of E and ν. Moreover, by substituting $D_r = 0$ in Eq. (S4), we immediately obtain the following equation:

$$\dot{\varphi} = \varepsilon_{rr}^{-1}(e_{rr}\dot{u} + 2e_{r\theta}\frac{u}{r})\,. \tag{S7}$$

Let us finally remark that we end up with Eq. (S1) as the main governing equation, to be solved for the unknown u, so as to subsequently obtain φ by integrating Eq. (S7).

Model solution

By using Eq. (S2-S3) and Eq. (S7), we firstly recast Eq. (S1) as follows:

$$\ddot{u} + 2\frac{\dot{u}}{r} + \lambda\frac{u}{r^2} = 0\,, \tag{S8}$$

where

$$\lambda \equiv 2\frac{\alpha-\beta}{\gamma}\,, \tag{S9}$$

$$\alpha \equiv c_{r\theta} + \frac{e_{rr} e_{r\theta}}{\varepsilon_{rr}}, \tag{S10}$$

$$\beta \equiv c_{\theta\theta} + c_{\theta\phi} + 2\frac{e_{r\theta}^{\ 2}}{\varepsilon_{rr}}, \tag{S11}$$

$$\gamma \equiv c_{rr} + \frac{e_{rr}^{\ 2}}{\varepsilon_{rr}}. \tag{S12}$$

Then, by recalling standard techniques, we look for solutions of the form $u = \tilde{u} r^s$, so that s is a root of the characteristic equation $s^2 + s + \lambda = 0$. In our case $\lambda < 0$; this can be verified by using the parameter values reported below, and could be guessed by observing that $\lambda = -2$ for the purely elastic case ($e_{rr} = e_{r\theta} = 0$). Hence, the characteristic equation has two real roots, one positive and one negative. By discarding the negative root (to avoid the singularity at $r = 0$), we obtain:

$$u = \tilde{u} r^s, \tag{S13}$$

with

$$s \equiv \frac{\sqrt{1-4\lambda} - 1}{2}. \tag{S14}$$

Finally, we determine the unknown constant $\tilde{u}$ by exploiting the pressure boundary condition: once substituted Eq. (S13) in Eq. (S2), we impose $\sigma_r(r = R) = -p_{US}$, so as to finally obtain

$$u = u_R \left(\frac{r}{R}\right)^s, \tag{S15}$$

where

$$u_R \equiv -R\left(\frac{p_{US}}{s\gamma + 2\alpha}\right) \tag{S16}$$

denotes the maximum (inward) displacement, occurring on the NP surface. It is worth observing that Eq. (S16) correctly reduces to the classical solution $-R(1-2\nu)(\frac{p_{US}}{E})$ when considering the purely elastic case.[S10]

After substituting the solution provided by Eq. (S15), it is straightforward to integrate Eq. (S7) so as to obtain the following expression for the electric potential:

$$\varphi = \varphi_R(\frac{r}{R})^s, \tag{S17}$$

where

$$\varphi_R \equiv -\frac{R(se_{rr}+2e_{r\theta})}{s\varepsilon_{rr}}\left(\frac{p_{US}}{s\gamma+2\alpha}\right) \tag{S18}$$

denotes the maximum voltage difference, taking place on the NP surface. We fixed the arbitrary integration constant by setting $\varphi(r = 0) = 0$; this way, φ_R provides the electric potential increment taking place on the NP surface ($r = R$) with respect to the stress-free condition for the BTNP.

Voltage estimate

Let us now compute φ_R for a BTNP with radius $R = 1.5\cdot10^{-7}$ m, by exploiting Eq. (S18). To the purpose, we obtain the elastic constants from Eq. (S5-S6) by adopting $E \cong 70$ GPa[S5-S6] and $\nu = \frac{1}{3}$.[S4] Moreover, the piezoelectric coefficients are $e_{rr} \approx 10$ C/m^2 and $e_{r\theta} \approx -1$ C/m^2.[S4, S11-S12] Furthermore, the relative dielectric constant (*i.e.*, $\frac{\varepsilon_{rr}}{\varepsilon_0}$, where $\varepsilon_0 \cong 8.85\cdot10^{-12}$ F/m is the vacuum dielectric constant) is in the range 10^2 - 10^3,[S4, S12-S13] the extremes of which are derived from the ones of (crystal) bulk barium titanate. However, a relative dielectric constant slightly below 10^2

was measured specifically addressing thin films (thickness on the order of 100 nm).[S13] Hence, we assume $\frac{\varepsilon_{rr}}{\varepsilon_0} \approx 5 \cdot 10^2$ (yet keeping in mind that 10^2 might be a reasonable estimate as well).

Furthermore, we compute the maximum stimulation pressure as $p_{US} = \sqrt{2 I_{US} Z_W}$, where Z_W denotes the impedance of water, and I_{US} represents the ultrasound intensity (directly controlled during the experiments). In more detail, $Z_W = \rho_W c_W$, where $\rho_W \cong 10^3$ kg/m^3 denotes the water density and $c_W \cong 1.5 \cdot 10^3$ m/s is the sound speed in water. Furthermore and with reference to the carried out tests, we consider both $I_{US} = 10^3$ W/m^2 and $I_{US} = 8 \cdot 10^3$ W/m^2 (*i.e.*, 0.1 and 0.8 W/cm^2).

According to Eq. (S18), when stimulating with 0.1 W/cm^2 the maximum voltage is $\varphi_R \approx 0.07$ mV, while we get $\varphi_R \approx 0.19$ mV when operating with 0.8 W/cm^2 (and these voltages respectively become 0.29 and 0.82 mV when assuming 10^2 as relative dielectric constant).

Based on the above estimate, when using 0.8 W/cm^2, the local voltage on those regions on the cell membrane where BTNPs cluster (from confocal images clusters of about 10 BTNPs in average have been quantified) can affect the open probability of the voltage-gated channels. Conversely, when using 0.1 W/cm^2, it is likely that the local voltage does not modify channel open probability to produce a detectable response, not even close to the BTNP clusters.

Of course, we obtained the above estimate in a simplified modeling framework. For instance, the local value of the electric potential also depends on the cluster structure, and accurate computations should be performed based on more refined physical approximations. However, in the absence of a deeper characterization of the involved physical effects (starting with the relevant NP properties), our approach seems to be fully commensurate with the available data and with the model objective.

Moreover and quite remarkably, the above model predictions are fully compatible with the experimental observations. Hence, despite its inherent simplifications, our simple approach takes a first – yet quantitative – step toward the study of piezoelectric NP-assisted cell stimulation by ultrasounds.

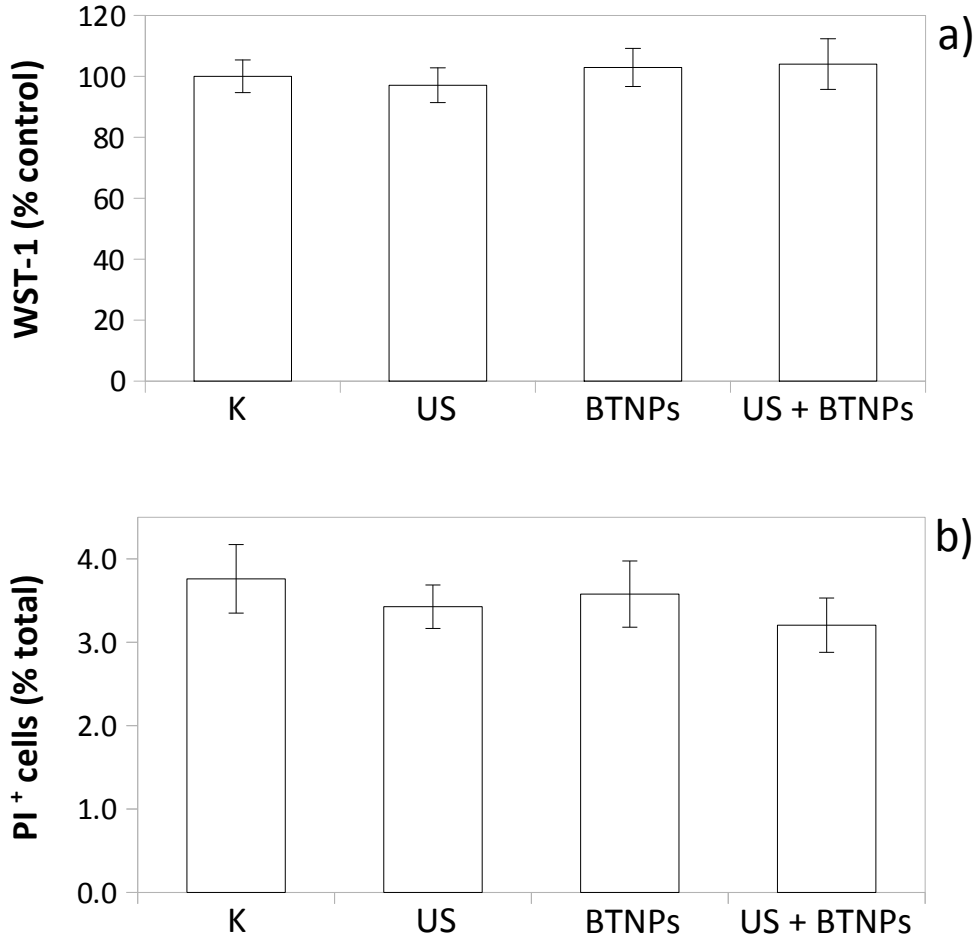

Figure S1. Evaluation of potential harmful effects of the proposed stimulation approach on SH-SY5Y cells. Metabolic activity (a) and membrane integrity (b) of cells exposed to US, BTNPs, or US + BTNPs compared to control cultures (K). WST-1 was performed after 24 h since the stimulation, propidium iodide (PI) staining immediately after the stimulation.

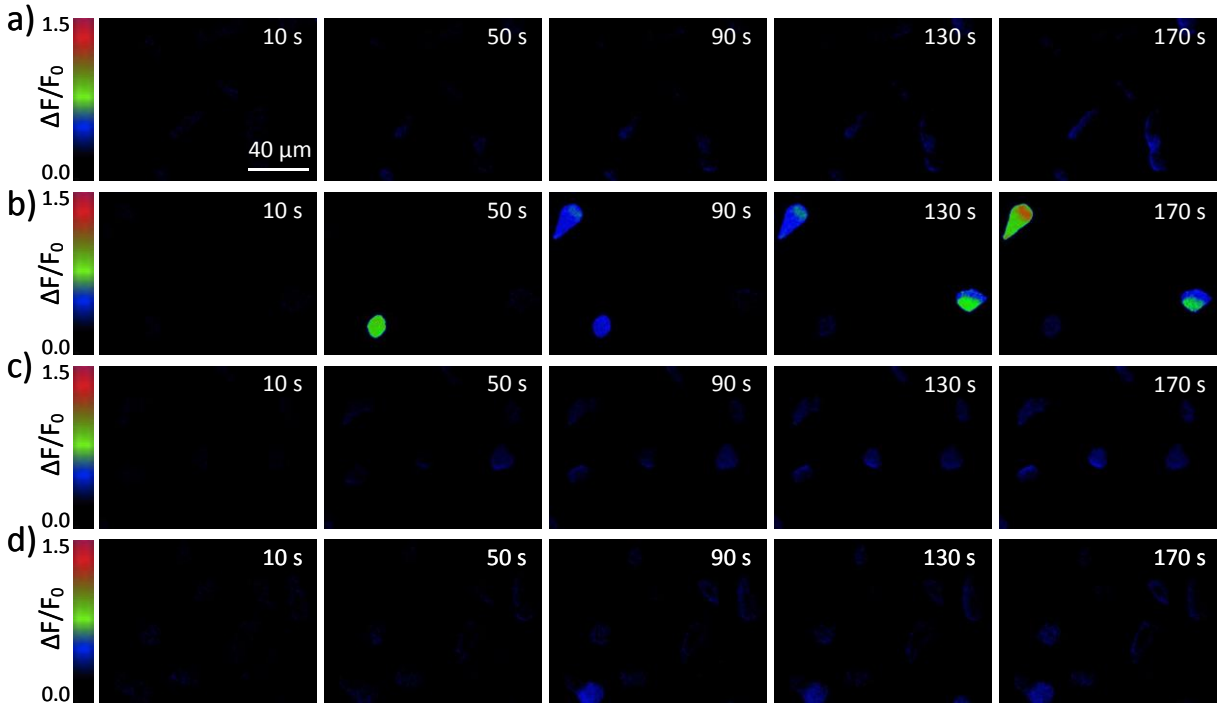

Figure S2. The US + BTNP stimulation (0.8 W/cm^2) evokes Cd^{2+} and TTX-sensitive calcium transients. Representative calcium imaging time-lapses of SH-SY5Y-derived neurons stimulated by US (a), US + BTNPs (b), US + BTNPs in the presence of Cd^{2+} (c) or TTX (d). The 5-s US stimulation was applied at 18 s.

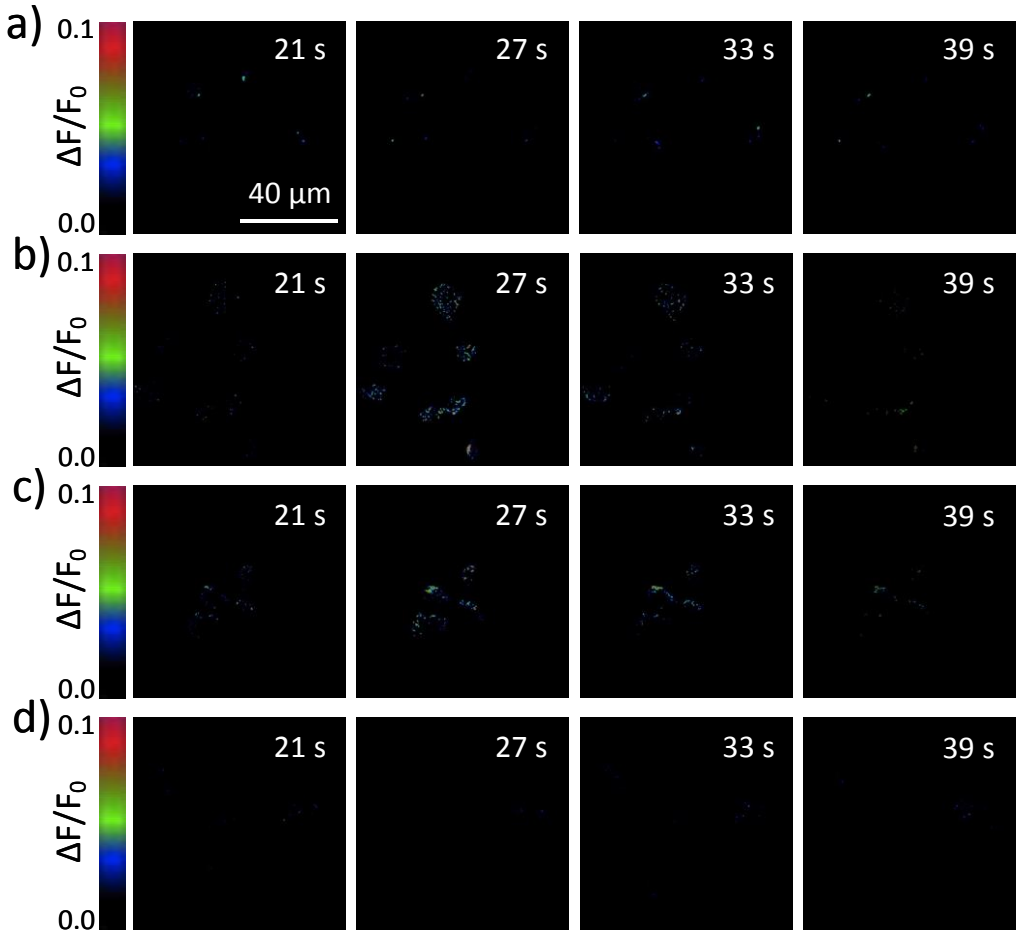

Figure S3. The US + BTNP stimulation (0.8 W/cm^2) induces TTX-sensitive sodium transients. Representative sodium imaging time-lapses of SH-SY5Y-derived neurons stimulated by US (a), US + BTNPs (b), US + BTNPs in the presence of Cd^{2+} (c) or TTX (d). The 5-s US stimulation was applied at 24 s.

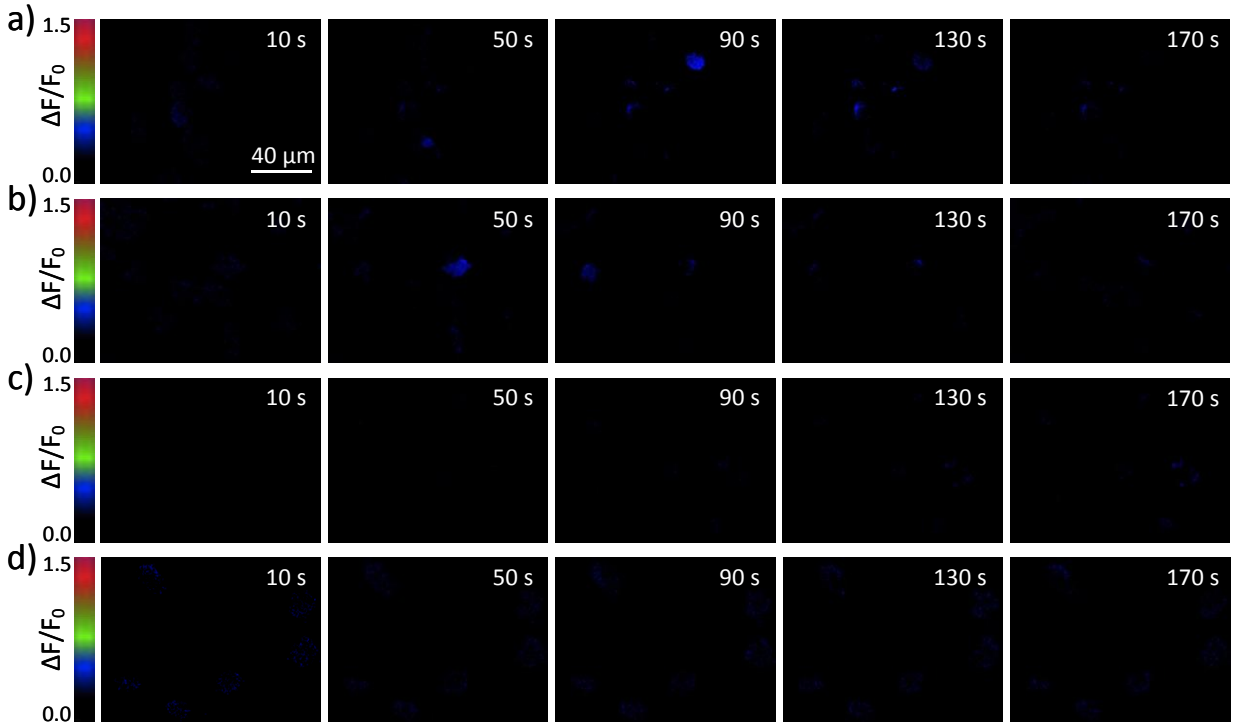

Figure S4. Calcium sources involved during US and US + BTNP stimulations (0.8 W/cm^2). Representative calcium imaging time-lapses of SH-SY5Y-derived neurons in calcium-free conditions stimulated by US (a) and US +BTNPs (b) show in both cases low-amplitude calcium transients. Observed transients were completely hindered by depleting the Ca^{2+} flux from the endoplasmic reticulum with thapsigargin before both the US (c) and US + BTNP (d) stimulations. The 5-s US stimulation was applied at 20 s.

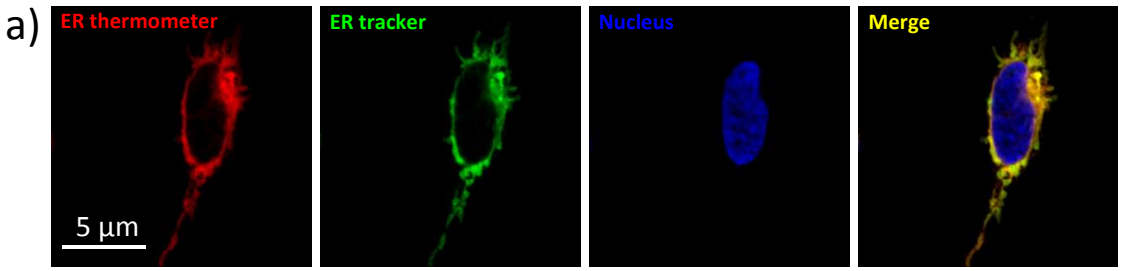
a)
ER thermometer
ER tracker
Nucleus
Merge
5 µm

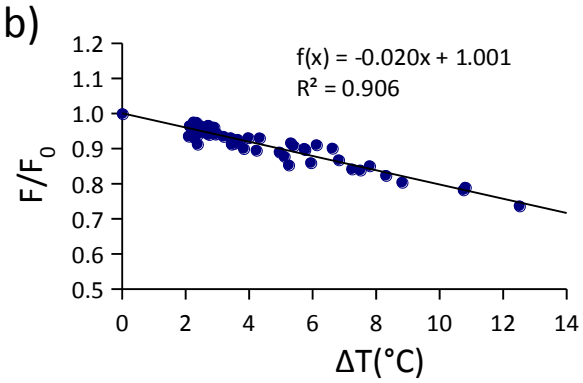
b)
f(x) = -0.020x + 1.001
R² = 0.906
F/F0
ΔT(°C)

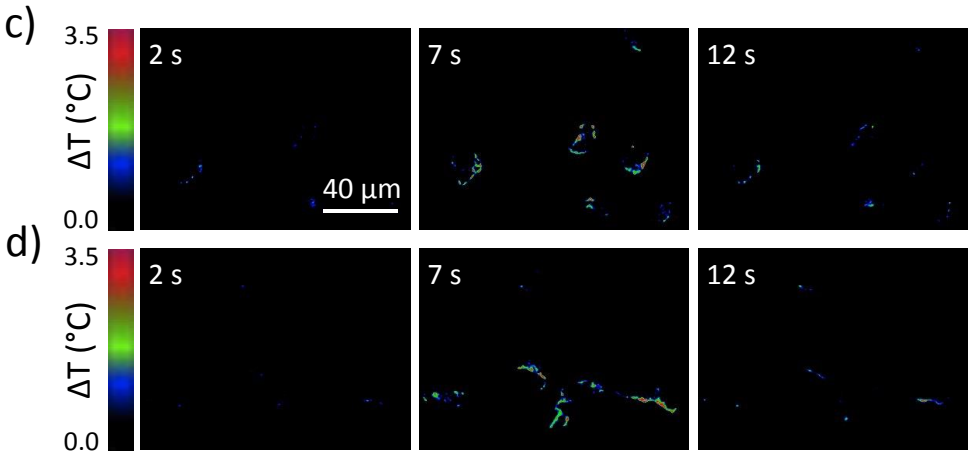
c)
d)
ΔT (°C)
2 s
7 s
12 s
40 µm

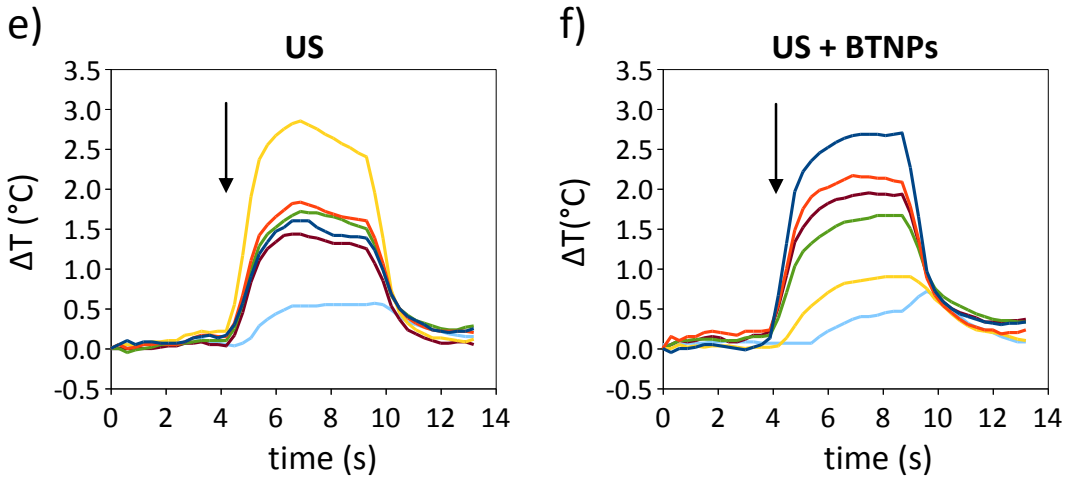
e)
US
f)
US + BTNPs
ΔT (°C)
ΔT(°C)
time (s)

Figure S5. US (0.8 W/cm^2) stimulation increases the temperature of the ER independently from the presence of the BTNPs. (a) Specific targeting of the fluorescent nano-thermometer (in red) to the endoplasmic reticulum (ER, stained in green with the ER tracker); nuclei are counter-stained in blue; the merged image shows the co-localization of the ER thermometer and the ER tracker signal. (b) Calibration curve of ER thermometer sensitivity, obtained by heating the ER applying a near infrared laser (1064 nm) at progressively shorter distances. The linear fitting of the F/F_0 values measured at different temperatures revealed an ER thermometer sensitivity of -2.0 %/°C. The temperature imaging time courses of the SH-SY5Y-derived neurons stimulated by US (c) and by US + BTNPs (d) show a comparable temperature increase. Arrows indicate the moment when the 5-s US pulse was initiated. In (e) and (f) traces relative to the temperature courses of the experiments depicted in (c) and (d) are respectively reported; each trace correspond to a single cell measurement in the representative fields.

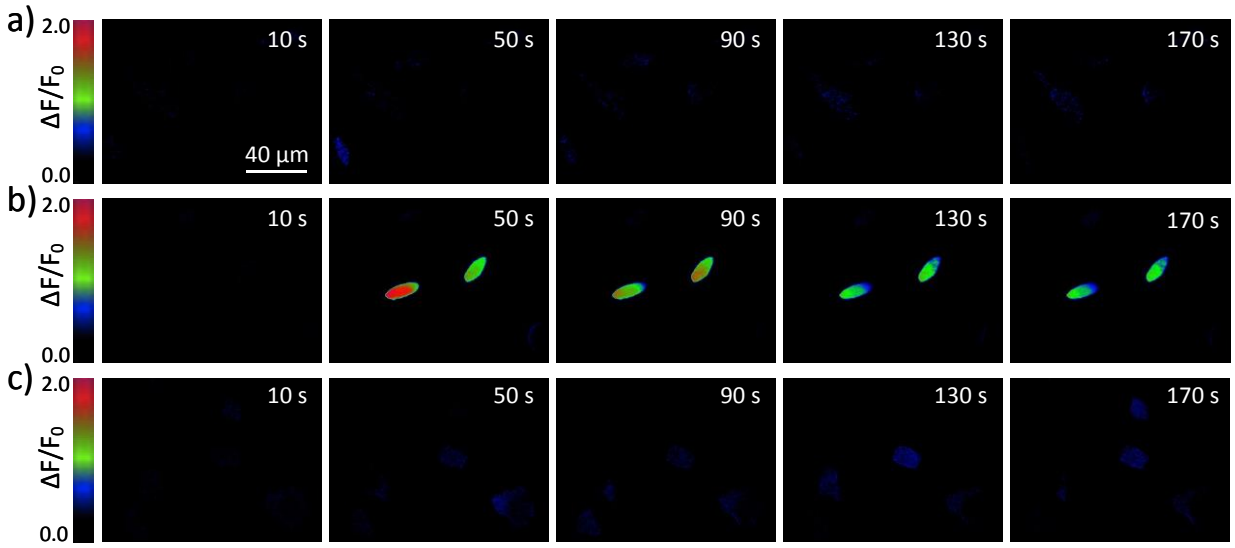

Figure S6. The calcium transients induced by US + BTNP stimulation (0.8 W/cm^2) are mediated by the piezoelectricity of the nanoparticles. Representative calcium imaging time-lapses of SH-SY5Y-derived neurons stimulated by US (a) and US +BTNPs (b) in the presence of gentamicin, a mechanoreceptor blocker which does not affect the voltage-gated Ca^{2+} currents. In (c) the Ca^{2+} time course of neurons stimulated by US and nonpiezoelectric BTNPs, characterized by a cubic crystalline configuration. The 5-s US stimulation was applied at 20 s.

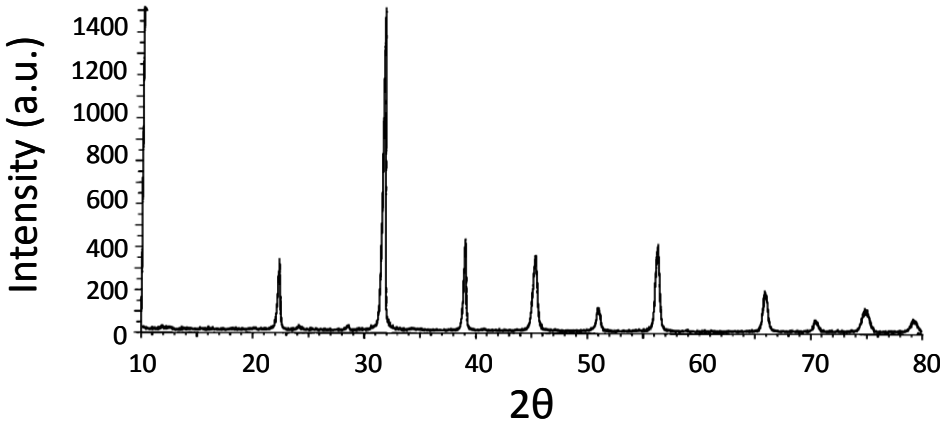

Figure S7. XRD crystallography of nonpiezoelectric BTNPs characterized by a cubic crystalline configurations: a single peak at $2\theta = 45°$ is highlighted.

Supporting references

S1. Catterall, W.A. Structure and Function of Voltage-Gated Ion Channels. *Annu. Rev. Biochem.* **1995**, *64*, 493–531.

S2. Hanukah, E.A New Closed-Form Model for Isotropic Elastic Sphere Including New Solutions for the Free Vibrations Problem. *arXiv preprint* **2013**, arXiv:1311.0741.

S3. Voisin, C.; Christofilos, D.; Del Fatti, N.; F. Vallée. Environment Effect on the Acoustic Vibration of Metal Nanoparticles. *Physica B* **2002**, *316–317*, 89–94.

S4. Dent, A.C.; Bowen, C.R.; Stevens, R.; Cain, M.G.; Stewart, M. Effective Elastic Properties for Unpoled Barium Titanate. *J. Eur. Ceram. Soc.* **2007**, *27*, 3739–3743.

S5. Wang, Z.; Hu, J.; Suryavanshi, A.P.; Yum, K.; Yu, M.F. Voltage Generation from Individual $BaTiO_3$ Nanowires under Periodic Tensile Mechanical Load. *Nano Lett.* **2007**, *7*, 2966-2969.

S6. Park, K.I.; Lee, M.; Liu, Y.; Moon, S.; Hwang, G.T.; Zhu, G.; Kim, J.E.; Kim, S.O.; Kim, D.K.; Wang, Z.L.; Lee, K.J. Flexible Nanocomposite Generator Made of $BaTiO_3$ Nanoparticles and Graphitic Carbons. *Adv. Mater.* **2012**, *24*, 2999–3004.

S7. Heyliger, P.; Wu, Y.C. Electroelastic Fields in Layered Piezoelectric Spheres. *Int. J. Eng. Sci.* **1999**, *37*, 143–161.

S8. Chen, W.Q. Problems of Radially Polarized Piezoelastic Bodies. *Int. J. Solids Struct.* **1999**, *36*, 4317–4332.

S9. Ghorbanpour Arani, A.; Kolahchi, R.; Mosallaie Barzoki, A.A.; Loghman A. Electro-Thermo-Mechanical Behaviors of FGPM Spheres Using Analytical Method and ANSYS Software. *App. Math. Model.* **2012**, *36*, 139–157.

S10. Landau, L.D.; Lifshitz, E.M. Theory of Elasticity (Volume 7 of "Course of Theoretical Physics"), Pergamon Press, Oxford, UK, 1970.

S11. Berlincourt, D.A.; Krueger H.H.A.; Near, C. Properties of Piezoelectric Ceramics. Technical Publication TP-226, Morgan Electro Ceramics Ltd., Wrexham, UK, 1999.

S12. Zgonik, M.; Bernasconi, P.; Duelli, M.; Schlesser, R.; Gunter, P.; Garrett, M.H.; Rytz, D.; Zhu, Y.; Wu X. Dielectric, Elastic, Piezoelectric, Electro-Optic, and Elasto-Optic Tensors of $BaTiO_3$ Crystals. *Phys. Rev. B*, **1994**, *50*, 5941–5949.

S13. Huang, L.; Chen, Z.; Wilson, J.D.; Banerjee, S.; Robinson, R.D.; Herman, I.P.; Laibowitz, R.; O'Brien, S. Barium Titanate Nanocrystals and Nanocrystal Thin Films: Synthesis, Ferroelectricity, and Dielectric Properties. *J. Appl. Phys.* **2006**, *100*, 034316.